Inorganica Chimica Acta 362 (2009) 1963–1968

Contents lists available at ScienceDirect

Inorganica Chimica Acta

journal homepage: www.elsevier.com/locate/ica

Interconversion between cyclodimer and cyclotrimer: Synthesis and characterization of *cyclo*-[Pd(II)Cl_2(N–N)] complexes

Hyun Ji Kang [a], Tae Hwan Noh [a], Young Mee Na [a], Kyung Ho Yoo [b], Ok-Sang Jung [a,*]

[a] Department of Chemistry, Pusan National University, Pusan 609-735, Republic of Korea
[b] Korea Institute of Science and Technology, Seoul 136-791, Republic of Korea

ARTICLE INFO

Article history:
Received 24 June 2008
Received in revised form 6 September 2008
Accepted 8 September 2008
Available online 20 September 2008

Keywords:
Cyclodimers
Cyclotrimers
Interconversion
Microspheres
Palladium(II) complexes

ABSTRACT

The reaction of (COD)$PdCl_2$ (COD = 1,5-cyclooctadiene) with (3-Py)$_2$SiR_1R_2 (3-Py = 3-pyridyl; R_1 = Ph, R_2 = Ph (*m*-pdps); R_1 = Ph, R_2 = Me (*m*-pmps)) in acetone affords single crystals consisting of cyclodimers, [$PdCl_2$((3-Py)$_2$SiR_1R_2)]$_2$, whereas the same reaction in a mixture of dichloromethane and ethanol yields amorphous spheres consisting of cyclotrimers, [$PdCl_2$((3-Py)$_2$SiR_1R_2)]$_3$. In a boiling chloroform solution, the cyclodimers are completely converted to cyclotrimers. These cyclotrimers, in the 10–60 °C range, are partly returned to cyclodimers. By contrast, the reaction of (COD)$PdCl_2$ with (3-Py)$_2$SiR_1R_2 (R_1 = Bu, R_2 = Me (*m*-pbms); R_1 = dodecyl, R_2 = Me (*m*-pddms)) yields amorphous spheres consisting of cyclotrimers irrespective of solvents. Both [$PdCl_2$(*m*-pbms)]$_3$ and [$PdCl_2$(*m*-pddms)]$_3$ are initially cyclotrimers in chloroform, but they exist as a mixture of cyclodimers and cyclotrimers in solution in the 10–60 °C range. The metallacycles tend to form cyclodimers in the order *m*-pdps > *m*-pmps > *m*-pbms > *m*-pddms. The equilibrium between cyclodimers and the cyclotrimers is sensitive to solvent, temperature, and concentration as well as molecular structure.

1. Introduction

Among diverse dynamic systems, those that can control macrocyclic rings by means of chemical triggers are of importance in the field of task-specific molecular materials. Thus, various metallamacrocycles have been synthesized as important building blocks in the construction of functional supramolecular materials that can be utilized for molecular machines, switches, recognition, selective transformation, drug delivery systems, catalysts, storage, and biomimics [1–10]. One of the facile synthetic systems is ring-expansion [11–14], which includes cavity-control [15,16] by means of labile metal–ligand coordination and thermodynamic control. Some palladium(II) complexes of N-donor ligands have been utilized in the development of coordination materials such as catalysts [17], rectangular building blocks [18], submicrospheres [19], desirable morphology [20], and "magic ring" with the associative/dissociative dual character Pd–N bond [21]. Of the N-donor ligands, silicon-containing pyridyl ligands have been found to be useful for the synthesis of targe-skeletal structures since they are adjustable in bridging ability and length, possess flexible angles around silicon, and are conformationally nonrigid [22–26]. Equilibria of ionic palladium(II) metallacyclic compounds containing NO_3^-, PF_6^-, or OTf^- have been observed [27,28], but ring-control in neutral palladium(II) complexes is very rare. Nonetheless, the facile manipulation of well-defined micro-shapes remains an important issue with regard to the development of advanced materials. Intermolecular affinity is the key factor in the formation of a particle-based morphology [29]. A comparative investigation of single crystals versus amorphous morphology still remains a keen challenge.

In this context, a preliminary result in morphology-control via the ring size of neutral metallamacrocyclic compounds has recently been published [30]. In order to expand the systematic tendency to form cyclodimers/cyclotrimers according to the organic chains attached to silicon as well as the external conditions, we report the formation and interconversion processes of metallacyclodimers versus metallacyclotrimers.

2. Experimental

2.1. Materials and measurements

Palladium(II) chloride, 1,5-cyclooctadiene (COD), and various dialkyldichlorosilanes were purchased from Aldrich, and used without further purification. (COD)$PdCl_2$ was prepared according to the procedure described in the literature [31]. Bis(3-pyridyl)dodecylmethylsilane (*m*-pddms) [32] and [$PdCl_2$(*m*-pmps)] (*m*-pmps = bis(3-pyridyl)methylphenylsilane) [30] were prepared according to the previous studies. The ^{1}H and ^{13}C NMR spectra were recorded on a Varian Gemini 300, the chemical shifts of which were relative to the internal $SiMe_4$. Infrared spectra were

* Corresponding author. Tel.: +82 51 510 2591; fax: +82 51 516 7421.
E-mail address: oksjung@pusan.ac.kr (O.-S. Jung).

0020-1693/$ - see front matter © 2008 Published by Elsevier B.V.
doi:10.1016/j.ica.2008.09.024

obtained on a Perkin Elmer 16F PC FTIR spectrophotometer with samples prepared as KBr pellets. Elemental microanalyses (C, H, N) were performed on solid samples in the Advanced Analytical Division at KBSI, using a Perkin Elmer 2400 CHNS analyzer. Thermal analyses were performed under a nitrogen atmosphere at a scan rate of 10 °C/min with a Stanton Red Croft TG 100. Mass spectrometric analysis via a fast atom bombardment technique was performed in chloroform using a KMS-700 Mstation mass spectrometer (Jeol, Japan) and an MS-MP9020D data system.

2.2. Synthesis of bis(3-pyridyl)diphenylsilane (m-pdps)

n-Butyllithium (14.4 mmol, 2.5 M solution in hexane) was added dropwise to a solution of 3-bromopyridine (14 mmol) in dry ethyl ether (40 ml) under nitrogen gas at −78 °C, at which temperature the resulting mixture was stirred for 1 h. At 0 °C, dichlorodiphenylsilane (6.5 mmol) was slowly added to the yellow suspension over 2 h. Distilled water (20 ml) was added into the reaction solution, and the organic solution layer was separated. The organic solution was washed with water (2 × 10 ml), and then was dried over $MgSO_4$. The crude product was purified by column chromatography on silica gel with ethyl acetate. The solvent was evaporated to obtain a pale yellow solid in 60% yield. ^{1}H NMR ($CDCl_3$, $SiMe_4$, ppm): 7.27 (t, J = 6.3 Hz, 2H), 7.36–7.44 (m, 10H), 7.76 (dt, J = 7.5 Hz, J = 1.6 Hz, 2H), 8.70 (dd, J = 6.3 Hz, J = 1.4 Hz, 2H), 8.75 (s, 2H). ^{13}C NMR ($CDCl_3$, $SiMe_4$, ppm): 123.66, 128.58, 128.92, 130.64, 131.94, 136.42, 143.98, 151.20, 156.57.

2.3. Synthesis of bis(3-pyridyl)butylmethylsilane (m-pbms)

A similar reaction was carried out using *n*-butylmethyldichlorosilane instead of dichlorodiphenylsilane. The solvent was evaporated to obtain a viscous liquid in 58% yield. ^{1}H NMR ($CDCl_3$, $SiMe_4$, ppm): 0.55 (s, 3H), 0.78–0.83 (t, J = 6.7 Hz, 3H), 1.03–1.08 (m, 2H), 1.27–1.32 (m, 4H), 7.21 (t, J = 6.2 Hz, 2H), 7.69 (dt, J = 7.4 Hz, J = 1.0 Hz, 2H), 8.54 (dd, J = 6.1 Hz, J = 1.0 Hz, 2H), 8.62 (s, 2H). ^{13}C NMR ($CDCl_3$, $SiMe_4$, ppm): −4.95, 13.20, 13.66, 25.68, 26.40, 123.38, 131.32, 142.02, 150.40, 154.52.

2.4. Synthesis of $[PdCl_2(m\text{-pdps})]_2$

An acetone solution (5 ml) of *m*-pdps (3.38 mg, 0.01 mmol) was slowly diffused into an acetone solution (5 ml) of $(COD)PdCl_2$ (2.85 mg, 0.01 mmol). The solvent of the reaction mixture was slowly evaporated to obtain pale yellow crystals suitable for X-ray single crystallography. M.p. 201 °C (dec). Anal. *Calc.* for $C_{44}H_{36}Cl_4N_4Pd_2Si_2$: C, 51.23; H, 3.52; N, 5.43. Found: C, 51.10; H, 3.55; N, 5.33%. ^{1}H NMR ($CDCl_3$, $SiMe_4$, ppm): 7.27 (t, J = 6.0 Hz, 4H), 7.41–7.56 (m, 20H), 7.73 (d, J = 7.5 Hz, 4H), 8.86 (d, J = 6.0 Hz, 4H), 9.70 (s, 4H). ^{13}C NMR ($CDCl_3$, $SiMe_4$, ppm): 124.86, 129.02, 129.57, 130.56, 131.40, 136.48, 145.90, 154.33, 160.35. Mass: m/e = 997.1 $[M_D-Cl]^+$ and 960.9 $[M_D-Cl-HCl]^+$.

2.5. Synthesis of $[PdCl_2(m\text{-pdps})]_3$

An ethanol solution (7 ml) of *m*-pdps (3.38 mg, 0.01 mmol) was slowly diffused into a dichloromethane solution (5 ml) of $(COD)PdCl_2$ (2.85 mg 0.01 mmol). Evaporation of the solvent afforded pale yellow spheres of $[Pd(m\text{-pdps})Cl_2]_3$ in 70% yield after 1 day. M.p. 278 °C (dec). Anal. *Calc.* for $C_{66}H_{54}Cl_6N_6Pd_3Si_3$: C, 51.23; H, 3.52; N, 5.43. Found: C, 51.20; H, 3.48; N, 5.38%. ^{1}H NMR ($CDCl_3$, $SiMe_4$, ppm): 7.3 (t, J = 5.7 Hz, 6H), 7.44–7.53 (m, 30H), 7.86 (d, J = 7.5 Hz, 6H), 8.87 (d, J = 5.7 Hz, 6H), 8.90 (s, 6H). ^{13}C NMR ($CDCl_3$, $SiMe_4$, ppm): 124.88, 125.16, 129.03, 129.08, 129.55, 130.57, 130.68, 131.46, 136.50, 145.91, 146.44, 154.33, 154.76, 159.56, 160.34. Mass: m/e = 1513.1 $[M_T-Cl]^+$, 1317.0 $[M_T-Cl-HCl-Ph]^+$, 1173.9 $[M_T-Cl-HCl]^+$, and 1138.5 $[M_T-L-Cl-HCl]^+$.

2.6. Synthesis of $[PdCl_2(m\text{-pbms})]_3$

An ethanol solution (7 ml) of *m*-pbms (2.56 mg, 0.01 mmol) was slowly diffused into a dichloromethane solution (5 ml) of $(COD)PdCl_2$ (2.85 mg, 0.01 mmol). Slow evaporation of the solvent produced pale yellow spheres of $[Pd(m\text{-pbms})Cl_2]_3$ in 70% yield after 2 days. M.p. 195 °C (dec). Anal. *Calc.* for $C_{45}H_{60}Cl_6N_6Pd_3Si_3$: C, 41.54; H, 4.65; N, 6.46. Found: C, 41.30; H, 4.55; N, 6.66%. ^{1}H NMR ($CDCl_3$, $SiMe_4$, ppm): 0.69 (s, 9H), 0.913 (m , 9H), 1.06–1.28 (m, 6H), 1.30–1.52 (m, 12H), 7.32 (t, J = 6.3 Hz, 6H), 7.77 (d, J = 6.6 Hz, 6H), 8.85 (d, J = 6.3 Hz, 6H), 8.90 (s, 6H). ^{13}C NMR ($CDCl_3$, $SiMe_4$, ppm): −4.78, 12.97, 13.89, 25.60, 26.59, 125.18, 133.11, 144.88, 154.37, 157.90. Mass: m/e = 1187.7 $[M_T-3HCl]^+$, 1079.0 $[M_T-6HCl]^+$, 1009.2 $[M_T-L-HCl]^+$, 896 $[M_T-L-4HCl]^+$.

2.7. Synthesis of $[PdCl_2(m\text{-pddms})]_3$

An ethanol solution (7 ml) of *m*-pddms (3.68 mg, 0.01 mmol) was slowly diffused into a dichloromethane solution (5 ml) of $(COD)PdCl_2$ (2.85 mg, 0.01 mmol). Slow evaporation of the solvent afforded thin yellow powders of $[PdCl_2(m\text{-pddms})]_3$ in 70% yield after 2 days. M.p. 168 °C. Anal. *Calc.* for $C_{69}H_{108}Cl_6N_6Pd_3Si_3$: C, 50.60; H, 6.65; N, 5.13. Found: C, 51.40; H, 6.55; N, 5.08%. ^{1}H NMR ($CDCl_3$, $SiMe_4$, ppm): 0.68–1.58 (m, 84H), 7.34 (t, J = 6.6 Hz, 6H), 7.77 (d, J = 7.5 Hz, 6H), 8.86(d, J = 6.6 Hz, 6H), 8.91 (s, 6H). ^{13}C NMR ($CDCl_3$, $SiMe_4$, ppm): −4.82, 13.27, 14.38, 22.92, 23.54, 29.40, 29.58, 29.78, 29.88, 32.14, 33.64, 125.16, 133.15, 144.87, 154.38, 157.88. Mass: m/e = 1608 $[M_T-Cl]^+$, 1233.8 $[M_T-L-HCl]^+$, and 1198.8 $[M_T-L-Cl-HCl]^+$.

2.8. Crystal structure determination

X-ray data were collected on a Bruker SMART automatic diffractometer with graphite-monochromated Mo Kα radiation (λ = 0.71073 Å) and a CCD detector at ambient temperature. Forty five frames of two-dimensional diffraction images were collected and processed to obtain the cell parameters and orientation matrix. The data were corrected for the Lorentz and polarization effects. The absorption effects were corrected using the empirical ψ-scan method. The structures were solved using the direct method (SHELXS 97) and refined by full-matrix least squares techniques (SHELXL 97) [33]. The non-hydrogen atoms were refined anisotropically, and the hydrogen atoms were placed in calculated positions and refined only for the isotropic thermal factors. The crystal parameters and procedural information corresponding to the data collection and structure refinement are listed in Table 1.

Table 1
Crystal data and structure refinement for $[PdCl_2(m\text{-pdps})]_2$

Formula	$C_{22}H_{18}Cl_2N_2PdSi$
M_w	515.77
Crystal system	Monoclinic
Space group	$C2/c$
a (Å)	17.9540(9)
b (Å)	13.9431(7)
c (Å)	19.0212(9)
β (°)	114.8390(10)
V (Å^3)	4321.2(4)
Z	8
μ (mm^{-1})	1.172
GOF on F^2	1.070
Final R indices [$I > 2\sigma(I)$]	R_1 = 0.0238, wR_2 = 0.0641
R indices (all data)[a]	R_1 = 0.0299, wR_2 = 0.0667

[a] $R_1 = \sum ||F_o| - |F_c|| / \sum |F_o|$. $wR_2 = \sum w(F_o^2 - F_c^2)^2 / \sum wF_o^2)^{1/2}$.

3. Results and discussion

3.1. Synthesis

The reaction of $(COD)PdCl_2$ with the present ligands at room temperature yielded discrete cyclic compounds, as shown in Scheme 1. The reaction of $(COD)PdCl_2$ with *m*-pdps or *m*-pmps [30] in acetone yielded single crystals suitable for X-ray single crystallography, whereas the reaction in a mixture of dichloromethane and ethanol produced amorphous microspheres. When the single crystals were treated in a mixture of dichloromethane and ethanol, the same microspheres formed. Furthermore, recrystallization of the microspheres in acetone yielded single crystals. The single crystal consisted of cyclodimers whereas the amorphous microsphere consisted of cyclotrimers, as will be discussed in detail. Thus, the cyclodimers and the cyclotrimers could be smoothly isolated and interconverted. However, for the *m*-pbms and *m*-ddmps analogues, single crystals consisting of cyclodimers could not be isolated, instead amorphous microspheres were produced irrespective of solvents in contrast to above *m*-pdps or *m*-pmps analogues. $[PdCl_2(m\text{-pbms or } m\text{-pddms})]_2$ and $[PdCl_2(m\text{-pbms or } m\text{-pddms})]_3$ products existed in equilibrium in the solution. The equilibrium is sensitive to concentration and temperature. The reactions were originally conducted in the 1:1 mole ratio of Pd(II) to ligands, but the products were not significantly affected by the mole ratio. The present products are remarkable in that there was no evidence for polymerization, not even under high concentrations. All of the compounds are soluble in dichloromethane, chloroform, *N*,*N*-dimethylformamide, and dimethylsulfoxide, but are insoluble in water, hexane, ethanol, and nitromethane. The elemental analyses and NMR spectra of the products were consistent with desirable structures.

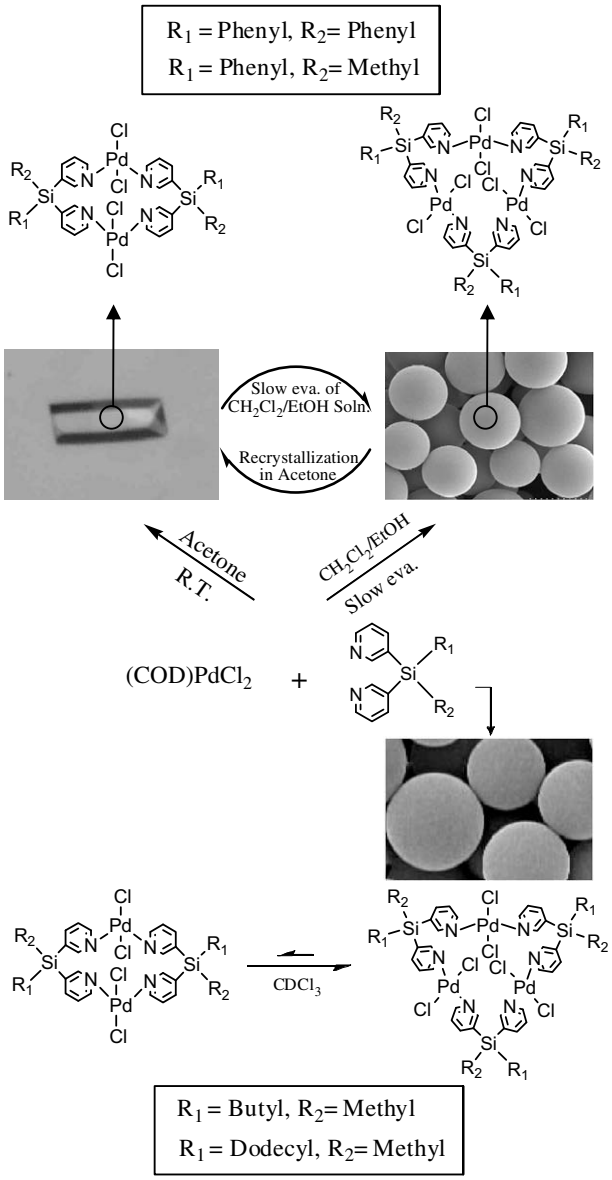

Scheme 1.

3.2. Crystal structure of $[PdCl_2(m\text{-pdps})]_2$

The crystal structure of $[PdCl_2(m\text{-pdps})]_2$ is illustrated in Fig. 1, and the relevant bond lengths and angles are listed in Table 2. The ORTEP shows that the single crystal consists of cyclodimers, $[PdCl_2(m\text{-pdps})]_2$. The local geometry around the palladium(II) ion approximates to a typical square planar arrangement with two chlorides in *trans* position (Cl–Pd–Cl = 174.67(2)°; N–Pd–N = 177.72(7)°; Pd–Cl = 2.2984(6) Å, 2.2874(6) Å; Pd–N = 2.045(2) Å, 2.007(2) Å). The *m*-pdps ligand connects two palladium(II) ions to form a 16-membered cyclodimer. The ligand acts as an unusual horse-shoe tectonic, which is useful for the construction of molecular rectangles [24]. The structure of $[PdCl_2(m\text{-pdps})]_2$ is a centrosymmetric molecule, in contrast to that of $[PdCl_2(m\text{-pmps})]_2$ [30]. The crystal consists of discrete cyclodimeric molecules with no close intermolecular contacts. No other exceptional features, including those of either bond lengths or angles, were observed.

3.3. NMR behavior and related properties

The ^1H NMR spectra of both the single crystal, $[PdCl_2(m\text{-pdps})]_2$, and the amorphous microsphere, $[PdCl_2(m\text{-pdps})]_3$, were measured in chloroform at room temperature (Fig. 2). The two spectra show a similar pattern, except for the chemical shifts of 2H-Py. The 2H-Py of $[PdCl_2(m\text{-pdps})]_3$ relative to that of $[PdCl_2(m\text{-pdps})]_2$ was significantly upfield-shifted, from 9.70 to 8.90 ppm. The cyclodimeric structure seems to be unusually rigid even in solution, and thus 2H-Py is strongly affected by the anisotropy effect. The weak interaction (C–H···Cl = 2.59 Å) can partly be ascribed to the downfield shift of 2H-Py in the cyclodimer. In contrast, for the cyclotrimer, the upfield shift of 2H-Py can be explained by the more fluxional motion of the pyridyl group. The FAB mass data for $[PdCl_2(m\text{-pdps})]_2$ and $[PdCl_2(m\text{-pdps})]_3$ (matrix: nitrobenzylalcohol) (Fig. 3) were obtained in order to characterize their chemical structures. The mass peaks of the amorphous microsphere (*m*/*e* = 1513.1 $[M_T–Cl]^+$, 1317.0 $[M_T–Cl–HCl–Ph]^+$, 1173.9 $[M_T–L–HCl]^+$, 1138.5 $[M_T–L–Cl–HCl]^+$; M_T = cyclotrimer) indicate

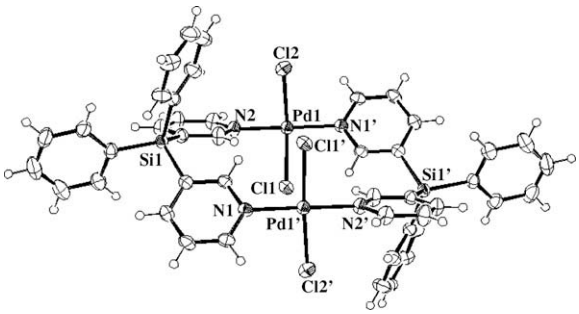

Fig. 1. X-ray structure of $[PdCl_2(m\text{-pdps})]_2$.

Table 2
Bond lengths (Å) and angles (°) for $[PdCl_2(m\text{-pdps})]_2$

Pd(1)–N(2)#1	2.0073(18)
Pd(1)–N(1)	2.0452(17)
Pd(1)–Cl(2)	2.2874(6)
Pd(1)–Cl(1)	2.2984(6)
N(2)–Pd(1)#1	2.0073(18)
N(2)#1–Pd(1)–N(1)	177.72(7)
N(2)#1–Pd(1)–Cl(2)	87.76(6)
N(1)–Pd(1)–Cl(2)	91.27(5)
N(2)#1–Pd(1)–Cl(1)	88.13(6)
N(1)–Pd(1)–Cl(1)	92.71(5)
Cl(2)–Pd(1)–Cl(1)	174.67(2)
C(1)–N(1)–Pd(1)	121.83(14)
C(5)–N(1)–Pd(1)	120.39(14)
C(21)–N(2)–Pd(1)#1	124.08(15)
C(22)–N(2)–Pd(1)#1	117.46(15)

Symmetry transformations used to generate equivalent atoms: #1 $-x, -y+1, -z$.

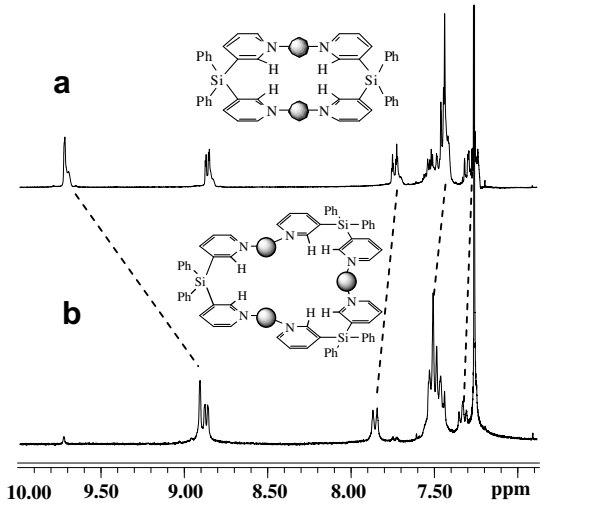

Fig. 2. ^{1}H NMR spectra of $[PdCl_2(m\text{-pdps})]_2$ (a) and $[PdCl_2(m\text{-pdps})]_3$ (b). ● indicates $PdCl_2$.

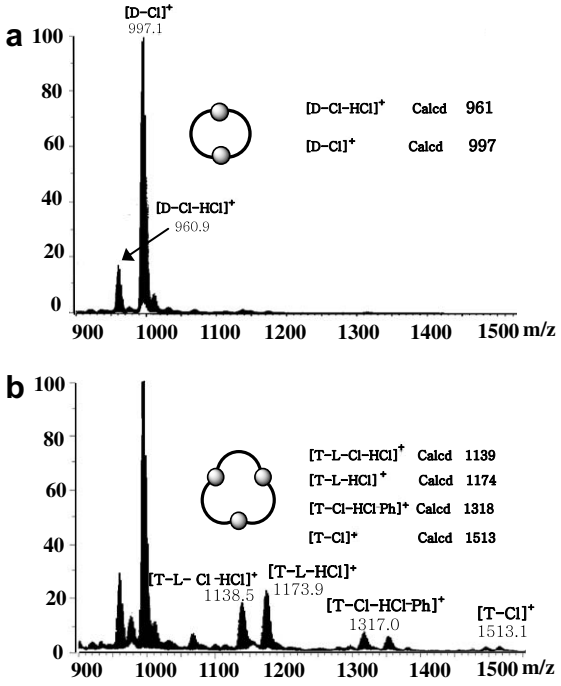

Fig. 3. FAB mass data for $[PdCl_2(m\text{-pdps})]_2$ (a) and $[PdCl_2(m\text{-pdps})]_3$ (b).

that it consists of cyclotrimers; the mass data for the single crystal show that it consists of cyclodimers (m/e = 997.1 $[M_D-Cl]^+$, 960.9 $[M_D-Cl-HCl]^+$; M_D = cyclodimer). Of course, conducting similar elemental analyses of the two compounds (C, H, N) was satisfactory. Furthermore, the cyclotrimers in chloroform at the 60 °C transformed them into cyclodimers (Fig. 4). Another interesting feature is that in the 10–60 °C range, the cyclotrimer partly returns to the cyclodimer in solution. Both the cyclodimer and the cyclotrimer are locked in the solution below 10 °C. The equilibria in the 10–60 °C range are dependent on temperature and concentration. High concentration favors the cyclotrimer. For $[PdCl_2(m\text{-pbms})]_3$ and $[PdCl_2(m\text{-pddms})]_3$, the ^{1}H NMR data show that they are initially cyclotrimers in chloroform (see the mass data for $[PdCl_2(m\text{-pbms})]_3$ and $[PdCl_2(m\text{-pddms})]_3$: Supplementary material S7). The two peaks of 2H-Py arose from the unsymmetricity via the presence of two significantly different organic groups. As time passes, these groups exist as a mixture of cyclodimers and cyclotrimers in the 10–60 °C range (Fig. 5). However, complete interconversion from cyclotrimers to cyclodimers does not occur, in contrast to $[PdCl_2(m\text{-pdps})]$ and $[PdCl_2(m\text{-pmps})]$.

3.4. Formation of spheres

Slow evaporation of $(COD)PdCl_2$ (0.01 mmol in 5 ml of CH_2Cl_2) with each ligand (0.01 mmol in 7 ml of EtOH) yielded microspheres, as shown in Fig. 6. Preliminary results on the formation and control of microspheres were published in our previous papers

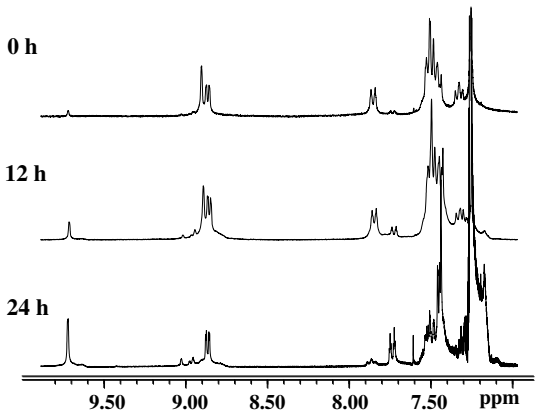

Fig. 4. ^{1}H NMR spectra for process of conversion from $[PdCl_2(m\text{-pdps})]_3$ to $[PdCl_2(m\text{-pdps})]_2$ in $CDCl_3$ at 60 °C.

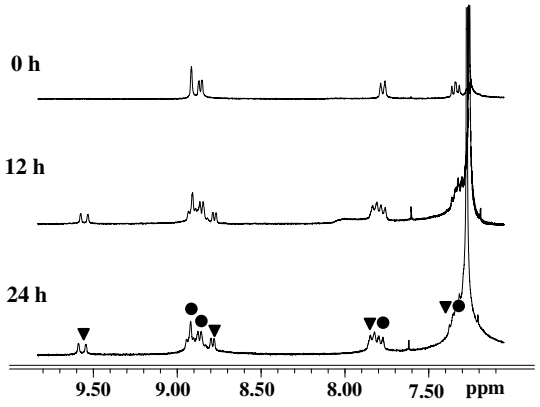

Fig. 5. Time-dependent ^{1}H NMR spectra for a process of conversion of $[PdCl_2(m\text{-pddms})]_3$ to $[PdCl_2(m\text{-pddms})]_2$ in $CDCl_3$ at 60 °C. (●: peaks from cyclotrimer; ▼: peaks from cyclodimer).

[30,34]. The SEM images show that the sphere-size is dependent on the organic groups attached to Si. The sphere-size of $[PdCl_2(m\text{-pdps})]_3$ (500 nm–1 μm) is very similar to that of $[PdCl_2(m\text{-pmps})]_3$. However, the spheres of $[PdCl_2(m\text{-pbms})]_3$ and $[PdCl_2(m\text{-pddms})]_3$ ($5 \sim 7$ μm), with long aliphatic chains, are larger than $[PdCl_2(m\text{-pdps})]_3$ under the same external conditions. The formation of different sizes can be explained by the solubility in the organic solvents. That is, long chain compounds are the more soluble in organic solvents, and thus a small number of seeds form, resulting in the formation of larger spheres. By contrast, for less soluble compounds, a large number of seeds form, resulting in the formation of smaller spheres. Moreover, the sphere-size (300 nm–7 μm) can be controlled by the evaporation rate of the solvent. Fast evaporation of solvent for 1 min using a rotary evaporator affords ~300 nm diameter submicrospheres. The part around $Pd(II)Cl_2$ seems to be hydrophilic, and the ligand moiety with a long aliphatic chain seems to be hydrophobic. These amphiphilic properties apparently form, without any additive, amorphous microspheres. Generally, monomodal submicrospheres of metal oxides are formed with organic additives and/or templates to control the nucleation, growth, and alignment of inorganic morphology [35,36].

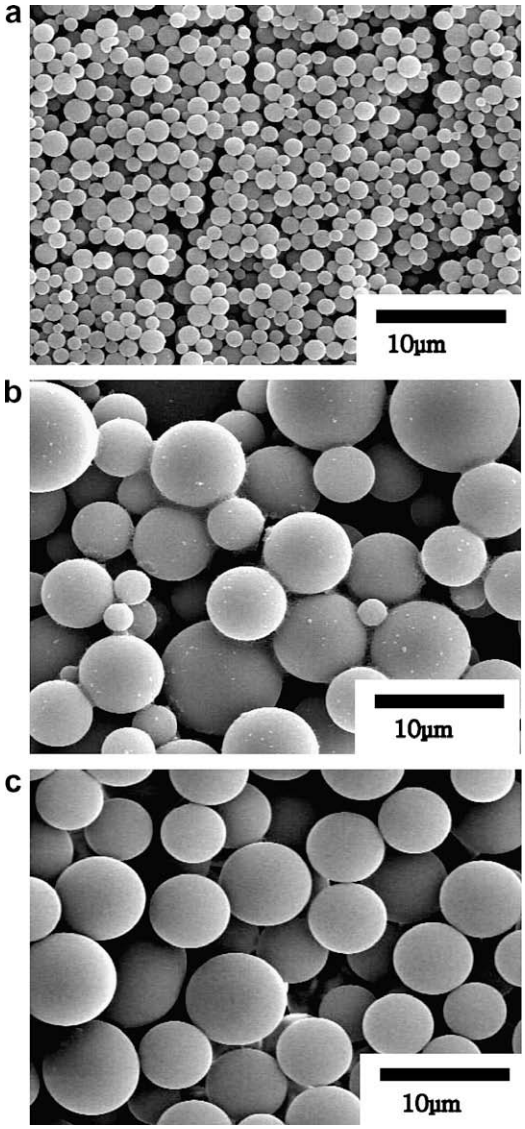

Fig. 6. SEM images of $[PdCl_2(m\text{-pdps})]_3$ (a), $[PdCl_2(m\text{-pbms})]_3$ (b) , and $[PdCl_2(m\text{-pddms})]_3$ (c).

3.5. Mechanistic aspect of interconversion

This system is an effective means of clearly showing the difference between the cyclodimer and the cyclotrimer. Indeed, the most significant difference between the two species, as established by the ^1H NMR spectra, is the molecular rigidity. The rigid cyclodimer produces single crystals, but the relatively fluxional cyclotrimer affords amorphous spheres. Furthermore, $[PdCl_2(m\text{-pbms})]_3$ and $[PdCl_2(m\text{-pddms})]_3$ with a long aliphatic chain cannot be obtained as single crystals in the solid state. That is, the complexes of the ligands containing the long aliphatic chains favor the cyclotrimers whereas the complexes of the ligands containing phenyl groups favor the cyclodimers in solution. Thus, the cyclodimer tends to form in the order *m*-pdps > *m*-pmps > *m*-pbms > *m*-pddms. The growth kinetics of solid products is determined by the interplay between the internal lattice structure and the external environment. Formation of spheres seems to be determined by a combination of surface tension, molecular flexibility, and solvent effects. Of course, the equilibrium between the cyclodimer and the cyclotrimer is sensitive to molecular structure, solvent, temperature, and concentration. Cyclodimer/cyclotrimer interconversion via temperature can be explained by the entropy difference between the two ($3\mathbf{D} \rightleftarrows 2\mathbf{T}$; $\Delta G^\circ = \Delta H^\circ - T\Delta S^\circ$). If *H* and *S* favor opposite processes, spontaneity will depend on temperature [37]. The formation of cyclotrimers is predominant above the chloroform reflux temperatures, meaning that the entropy of two cyclotrimer molecules is remarkably higher than that of three cyclodimer molecules in solution at high temperatures (ΔH° = positive; $T\Delta S^\circ$ = positive; $\Delta H^\circ < T\Delta S^\circ$; ΔG° = negative). However, in the 10–60 °C temperature range, ΔG° is positive because the ΔH° term is larger than the $T\Delta S^\circ$ term. Thus, the reverse reaction is a spontaneous (ΔH° = negative; $T\Delta S^\circ$ = negative; $\Delta H^\circ > T\Delta S^\circ$; ΔG° = positive) one below the reflux temperatures. The high entropy of the cyclotrimer is closely related both to the flexible NMR spectra and the formation of amorphous spheres. The cyclotrimer in chloroform below 0 °C is locked, indicating that the interconversion process requires somewhat higher activation energy. Thus, the conversion rate is slow.

4. Conclusions

The palladium(II) complexes of bidentate bis(3-pyridyl)dialkylsilane ligands are an effective system for explaining the relationship between molecular structure and physicochemical properties such as NMR behavior, morphology, temperature, and solvent. Such a control of morphology via the molecular ring size yields interesting results. Certainly, the structural rigidity of metal complexes will contribute to the development of molecular materials.

Acknowledgment

This work was supported financially by KOSEF R01-2007-000-20245-0 in Korea.

Appendix A. Supplementary material

CCDC 692358 contains the supplementary crystallographic data for this paper. These data can be obtained free of charge from The Cambridge Crystallographic Data Centre via www.ccdc.cam.ac.uk/data_request/cif. IR spectra of *m*-pdps (a), $[PdCl_2(m\text{-pdps})]_2$ (b), and $[PdCl_2(m\text{-pdps})]_3$ (c) (Fig. S1), IR spectra of *m*-pbms (a) and $[PdCl_2(m\text{-pbms})]_3$ (b) (Fig. S2), IR spectra of *m*-pddms (a) and

$[PdCl_2(m\text{-pddms})]_3$ (b) (Fig. S3), ^{13}C NMR spectra of *m*-pdps (a), $[PdCl_2(m\text{-pdps})]_2$ (b), and $[PdCl_2(m\text{-pdps})]_3$ (c) (Fig. S4), ^{13}C NMR spectra of *m*-pbms (a) and $[PdCl_2(m\text{-pbms})]_3$ (b) (Fig. S5), ^{13}C NMR spectrum of $[PdCl_2(m\text{-pddms})]_3$ (a) (Fig. S6), FAB mass data for $[PdCl_2(m\text{-pbms})]_3$ (a) and $[PdCl_2(m\text{-pddms})]_3$ (b) (Fig. S7), ^1H NMR spectra on a conversion process of $[PdCl_2(m\text{-pbms})]_3$ to $[PdCl_2(m\text{-pbms})]_2$ in $CDCl_3$ at 60 °C (Fig. S8). Supplementary data associated with this article can be found, in the online version, at doi:10.1016/j.ica.2008.09.024.

References

[1] G.F. Swiegers, T.J. Malefetse, Coord. Chem. Rev. 225 (2002) 91.
[2] F.A. Cotton, C. Lin, C.A. Murillo, Acc. Chem. Res. 34 (2001) 759.
[3] S. Leinigner, B. Olenyuk, P.J. Stang, Chem. Rev. 100 (2000) 853.
[4] H. Jude, H. Disteldorf, S. Fischer, T. Wedge, A.M. Hawkridge, A.M. Arif, M.F. Hawthorne, D.C. Muddiman, P.J. Stang, J. Am. Chem. Soc. 127 (2005) 12131.
[5] P. Wang, C.N. Moorefield, G.R. Newkome, Angew. Chem., Int. Ed. 44 (2005) 1679.
[6] Z. Grote, R. Scopelliti, K. Severin, J. Am. Chem. Soc. 126 (2004) 16959.
[7] K.D. Benkstein, J.T. Hupp, C.L. Stern, J. Am. Chem. Soc. 120 (1998) 12982.
[8] O.-S. Jung, Y.-A. Lee, Y.J. Kim, J. Hong, Cryst. Growth Des. 2 (2002) 497.
[9] K. Uehara, K. Kasai, N. Mizuno, Inorg. Chem. 46 (2007) 2563.
[10] Z. Zhang, R. Cai, Z. Chen, X. Zhou, Inorg. Chem. 46 (2007) 321.
[11] M. Fujita, M. Tominaga, A. Hori, B. Therrien, Acc. Chem. Res. 38 (2005) 369.
[12] N.C. Habermehl, D.J. Eisler, C.W. Kirby, N.L.-S. Yue, R.J. Puddephatt, Organometallics 25 (2006) 2921.
[13] M. Fujita, Chem. Soc. Rev. 27 (1998) 417.
[14] Y.M. Na, T.H. Noh, I.S. Chun, Y.-A. Lee, J. Hong, O.-S. Jung, Inorg. Chem. 47 (2008) 1391.
[15] J.R. Farrell, C.A. Mirkin, I.A. Guzei, L.M. Liable-Sands, A.L. Rheingold, Angew. Chem., Int. Ed. 37 (1998) 465.
[16] N.C. Gianneschi, M.S. Masar III, C.A. Mirkin, Acc. Chem. Res. 38 (2005) 825.
[17] Q. Yao, E.P. Kinney, C. Zheng, Org. Lett. 6 (2004) 2997.
[18] M. Fujita, F. Ibukuro, H. Hagihara, K. Ogura, Nature 367 (1994) 720.
[19] I.S. Chun, K.S. Lee, J. Do, Y. Hong, O.-S. Jung, Chem. Lett. (2007) 548.
[20] I.S. Chun, J.A. Kwon, H.J. Yoon, M.N. Bae, J. Hong, O.-S. Jung, Angew. Chem., Int. Ed. 46 (2007) 4960.
[21] S.R. Seidel, P.J. Stang, Acc. Chem. Res. 35 (2002) 972.
[22] O.-S. Jung, Y.J. Kim, K.M. Kim, Y.-A. Lee, J. Am. Chem. Soc. 124 (2002) 7906.
[23] O.-S. Jung, Y.-A. Lee, Y.J. Kim, Chem. Lett. (2002) 1906.
[24] O.-S. Jung, Y.J. Kim, Y.-A. Lee, S.W. Kang, S.N. Choi, Cryst. Growth Des. 4 (2004) 23.
[25] J.W. Lee, E.A. Kim, Y.J. Kim, Y.-A. Lee, Y. Pak, O.-S. Jung, Inorg. Chem. 44 (2005) 3151.
[26] M. Schmitz, S. Leninger, J. Fan, A.M. Arif, P.J. Stang, Organometallics 18 (1999) 4817.
[27] M. Fujita, O. Sasaki, T. Mitsuhashi, T. Fujita, J. Yajaki, K. Yamaguchi, K. Ogura, Chem. Commun. (1996) 1353.
[28] I.S. Chun, S.J. Moon, Y.M. Na, Y.-A. Lee, K.H. Yoo, O.-S. Jung, Inorg. Chem. Commun. 10 (2007) 967.
[29] H. Cölfen, S. Mann, Angew. Chem., Int. Ed. 42 (2003) 2350.
[30] H.J. Kang, T.H. Noh, J.S. Jin, O.-S. Jung, Inorg. Chem. 47 (2008) 5528.
[31] M.S. Kharasch, R.C. Seyler, F.R. Mayo, J. Am. Chem. Soc. 60 (1938) 882.
[32] S.A. Kim, J.P. Kim, Y.M. Ahn, J. Hong, O.-S. Jung, Bull. Korean Chem. Soc. 29 (2008) 729.
[33] G.M. Sheldrick, SHELXS-97: A Program for Structure Determination, University of Göttingen, Germany, 1997;
G.M. Sheldrick, SHELXL-97: A Program for Structure Refinement, University of Göttingen, Germany, 1997.
[34] S.A. Kim, H.J. Yoon, H.J. Kang, J.P. Kim, O.-S. Jung, Bull. Korean Chem. Soc. 29 (2008) 1266.
[35] H. Cölfen, M. Antonietti, Langmuir 14 (1998) 582.
[36] J.M. Marentette, J. Norwig, E. Stöckelmann, W.H. Meyer, G. Wegner, Adv. Mater. 9 (1997) 647.
[37] S.S. Zuhmdahl, S.A. Zuhmdahl, Chemistry, sixth ed., Houghton Mifflin, New York, 2003. p.795.